



Application of PALM Superresolution Microscopy to the Analysis of Microtubule-Organizing Centers (MTOCs) in *Aspergillus nidulans*

Xiaolei Gao, Reinhard Fischer, and Norio Takeshita

Abstract

Photoactivated localization microscopy (PALM), one of the super resolution microscopy methods improving the resolution limit to 20 nm, allows the detection of single molecules in complex protein structures in living cells. Microtubule-organizing centres (MTOCs) are large, multisubunit protein complexes, required for microtubule polymerization. The prominent MTOC in higher eukaryotes is the centrosome, and its functional ortholog in fungi is the spindle-pole body (SPB). There is ample evidence that besides centrosomes other MTOCs are important in eukaryotic cells. The filamentous ascomycetous fungus *Aspergillus nidulans* is a model organism, with hyphae consisting of multinucleate compartments separated by septa. In *A. nidulans*, besides the SPBs, a second type of MTOCs was discovered at septa (called septal MTOCs, sMTOC). All the MTOC components appear as big dots at SPBs and sMTOCs when tagged with a fluorescent protein and observed with conventional fluorescence microscopy due to the diffraction barrier. In this chapter, we describe the application of PALM in quantifying the numbers of individual proteins at both MTOC sites in *A. nidulans* and provide evidence that the composition of MTOCs is highly dynamic and dramatically changes during the cell cycle.

Key words PALM, *Aspergillus nidulans*, Ascomycete, Spindle pole body, Septal MTOC

1 Introduction

The filamentous fungus *Aspergillus nidulans* is an ideal model system to study the cell biology of lower eukaryotes due to the well-established toolboxes in genetics, biochemistry, cell biology and molecular biology. Many studies in *A. nidulans* focused on the analysis of polarity establishment, polar growth, or the function of the cytoskeleton [1–4]. Highlights were the discovery of γ -tubulin or the molecular analysis of cell cycle mutants [5–8]. The arrangement and interplay of the microtubule (MT) and the actin cytoskeletons is crucial for hyphal growth and the maintenance of polarity [9–11]. In *A. nidulans*, the MT cytoskeleton delivers the so-called cell-end marker proteins to the hyphal tips, which in turn polarize

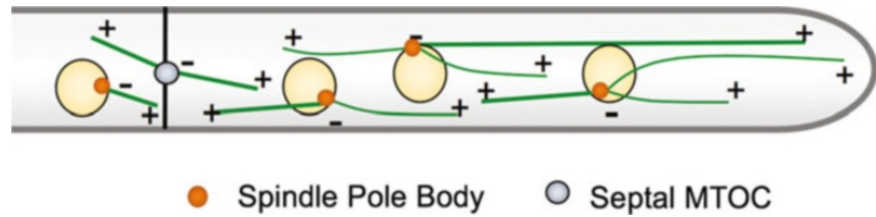


Fig. 1 Scheme of a hyphal compartment and the arrangement of MTOCs and MTs in *A. nidulans*. Hyphal compartments are separated by a septum and contain several nuclei. SPBs are the main MTOCs located at nuclei and septal MTOCs polymerize MTs bidirectionally from septa into the cytoplasm

the actin cytoskeleton [11, 12]. MTs are nucleated from large protein complexes, microtubule-organizing centers (MTOCs) in vivo. In *A. nidulans*, MTs are nucleated from at least two sites, the spindle-pole bodies (SPBs) which are embedded in the nuclear envelope and septal MTOCs (Fig. 1). Whereas the plus ends of MTs are highly dynamic, the minus ends are anchored at the MTOCs. The arrangement of MTOCs hence leads to a mixture of MT orientations in hyphal compartments, although in the tip region MTs are mainly oriented with their plus ends toward the apex (Fig. 1).

The simplest, but best characterized MTOC is the SPB of the budding yeast *Saccharomyces cerevisiae* which is a multilayered structure embedded into the nuclear envelope [13, 14]. The SPB is composed of at least 18 different proteins with a minimal complex for MT polymerization. This minimal complex is called γ -tubulin small complex (γ -TuSC) and consists of γ -tubulin plus two other γ -tubulin complex proteins (named GCP in humans). The protein names differ between organisms, because they were often discovered in mutagenesis approaches. In *S. cerevisiae* γ -tubulin is Tub2, GCP2 is Spc97 and GCP3 is Spc98 [15]. The fission yeast *Schizosaccharomyces pombe*, fungi like *A. nidulans*, and higher eukaryotes, contain a complex with more subunits GCP4, GCP5, and GCP6, which is called γ -tubulin ring complex (γ -TuRC). The understanding of γ -TuRC assembly into a spiral geometric structure for MTs nucleation is highly improved with cryo-electron microscopy reconstructions in a recent study of *Xenopus laevis* [16]. It highlights the significance of GCP6-specific insertion domain and actin as important structures of γ -TuRC. In *A. nidulans* MipA (γ -tubulin), GcpB and GcpC constitute the core γ -TuSC, and three additional GCPs GcpD, GcpE and GcpF are called γ -TuRC specific components or noncore components [17].

Although the SPB in *S. cerevisiae* and in *S. pombe* are very well studied, it was discovered that in *S. pombe* noncentrosomal MTOCs exist. Three different MTOCs were described, the spindle pole body, temporal MTOCs in the division plane (eMTOCs) and nuclear-envelope associated MTOCs in interphase cells (iMTOCs)

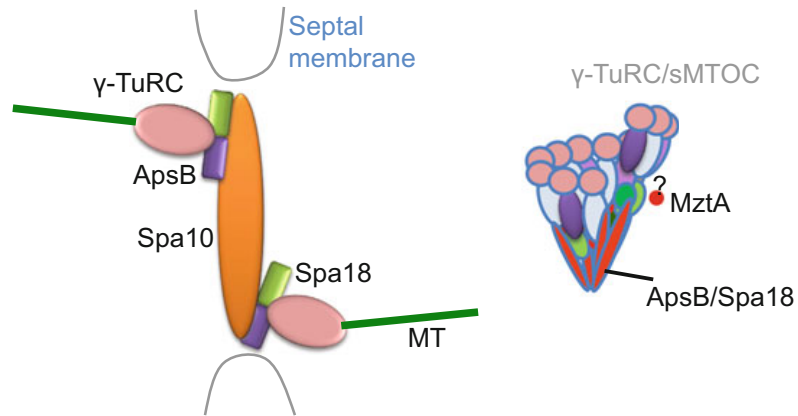


Fig. 2 Proposed model for septal MTOCs of *A. nidulans*. In the center of a mature septum Spa10 concentrates into a central disk structure and acts as an anchor for sMTOC components. ApsB interacts with Spa18 and both attach to the periphery of Spa10. From there they recruit γ -TuRCs and together polymerize microtubules (left, Adapted from [23]). Notably, γ -TuRC at septa contains GcpD, GcpE, GcpF, and MztA but with two outer plaque receptors ApsB and Spa18, defining a different structure from SPBs (right, Adapted from [22])

[18, 19]. We discovered that *A. nidulans* has two types of MTOCs, SPBs and septal MTOCs (sMTOCs). Although all γ -TuRC components were found at SPBs and at sMTOCs, other proteins were specific for the SPB or sMTOCs [20–23].

γ -TuRC is regulated by various factors that recruit it to different cellular sites, spatially controlling microtubule nucleation activities. In fission yeast, the outer plaque receptors of the γ -TuRC Mto1 and Mto2 play essential roles in nucleating cytoplasmic MTs, and the inner plaque receptor Pcp1 is responsible for spindle MTs nucleation [24–26]. Similarly, the outer plaque receptors of *A. nidulans*, ApsB^{Mto1} and Spa18^{Mto2}, were found to be at SPBs and sMTOCs and play essential roles for septal MTs nucleation [23]. At septa, an intrinsically disordered protein Spa10 was found to recruit ApsB and Spa18 (Fig. 2). At forming septa, Spa10 colocalized with the tropomyosin ring TpmA and at mature septa, where the actin ring disappeared, Spa10 concentrated into a stable central disk, while ApsB and Spa18 were only targeted to mature septa through attachment to the periphery of the Spa10 disk [23].

Recently, a new component of γ -TuRC was discovered in humans and named mitotic-spindle organizing protein associated with a ring of γ -tubulin (MOZART1) [27]. MOZART1 is conserved in most eukaryotes and its ortholog in *A. nidulans* is MztA. MztA interacted and colocalized with PcpA^{Pcp1}, the inner plaque receptor of the γ -TuRC, at SPBs. On the other hand, neither interaction nor colocalization was detected between MztA and ApsB [22]. MztA was also required to recruit GcpD and was located only at inner plaques of SPBs (Fig. 3). Taken together, the results suggested an asymmetry of the composition of the

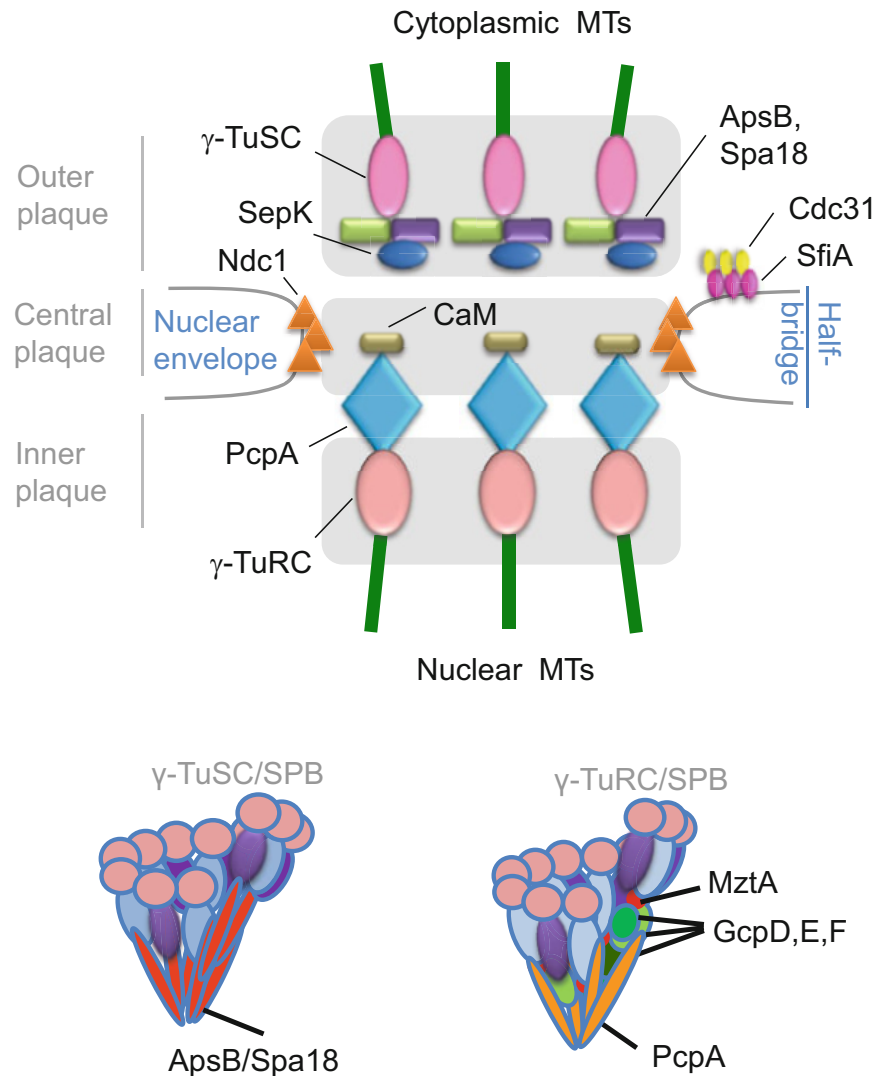


Fig. 3 Proposed model for the spindle pole body (SPB) of *A. nidulans*. The spindle pole body is composed of three plaques and a half bridge. The outer plaque harbours the small γ -TuSCs and the two receptor proteins ApsB and Spa18. The inner plaque harbours the big γ -TuRCs with MztA, and its receptor PcpA spans the central and inner plaque. SepK is one of the ApsB recruiters at the outer plaque. The only known component of the central plaque is CaM which binds to PcpA. Ndc1 is supposed to be a SPB component but its exact position still needs to be determined. Notably, it is not an anchor for SPBs. Cdc31 and Sfi1 are two orthologs of proteins resident at the half bridge and required for SPB duplication (Adapted from [22])

SPB in *A. nidulans*. Whereas the outer plaque of the SPBs is composed of γ -TuSCs, the inner plaque is composed of γ -TuRCs [22] (Fig. 3). Similarly, heterogeneity of γ -TuRCs was found in sperm cells of *Drosophila melanogaster* [28]. MztA was also found at sMTOCs in *A. nidulans* (Fig. 2,4). Hence, in *A. nidulans* three different MTOCs are established. The outer plaque with γ -TuSCs lacking MztA and the inner plaque with γ -TuRC containing MztA

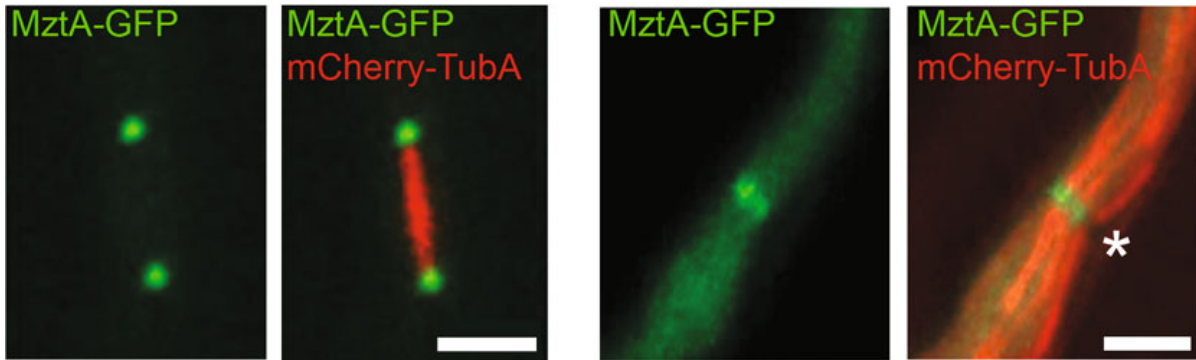


Fig. 4 Localization of MztA at SPBs and at sMTOCs as observed with epifluorescence microscopy in *A. nidulans*. MztA was fused to GFP and alpha tubulin (TubA) to mCherry. (Left) A single mitotic spindle with the two SPBs at their ends. (Right) Interphase MTs emanate from sMTOCs at septa. Asterisks indicate the septum position. Scale bar, 2 μ m (Adapted from [22])

(Fig. 3). sMTOCs appear to be hybrids of the two SPB MTOCs with γ -TuRCs including MztA (like the inner plaque) but with the anchor proteins ApsB and Spa18 (Fig. 2), which are typical components of the SPB outer plaques.

Using epifluorescence microscopy, all proteins of MTOCs in *A. nidulans* appeared as dots at SPBs and sMTOCs making it hard to resolve any further details of the molecular structures (Fig. 4). Light microscopy is restricted to an optical resolution of roughly 250 nm due to the diffraction limit [29]. Superresolution microscopy has been invented to bypass the physical barrier and enabled visualization of previously invisible molecular details in many biological systems [30]. Based on different principles of overcoming the diffraction limit, two categories of super-resolution approaches have been developed, (1) structured illumination microscopy (SIM) and stimulated emission depletion microscopy (STED) using patterned illumination to differently modulate the fluorescence emission, and (2) photoactivated localization microscopy (PALM) or stochastic optical reconstruction microscopy (STORM) by stochastically turning on individual molecular at different time points.

These methods have been applied to answer questions involving the organization, interaction, stoichiometry, and dynamics of cellular components. However, there are only a few applications of superresolution microscopy in filamentous fungi. One application of SIM in filamentous fungi is the localization of a STRIPAK subunit PRO45 at the nuclear envelope, endoplasmic reticulum, and mitochondria in *Sordaria macrospora* [31]. STED has revealed the size of lipid rafts to around 70 nm by visualizing flotillin FloA in *A. nidulans* [32, 33]. Expansion microscopy (ExM) is a sample preparation tool for biological samples that enables high-resolution imaging by expanding them using a polymer system on a conventional fluorescence microscopy [34]. This method was very recently applied to ascomycetes and basidiomycetes [35].

Here, we describe the application of photoactivated localization microscopy (PALM). It dramatically improves the spatial resolution to 10–20 nm [36, 37]. The basic principle behind PALM is the use of photoactivatable or photoconvertible fluorescent proteins to selectively switch on thousands of sparse subsets of molecules in a sequential manner. Most of the molecules are in an inactive state before a small fraction (less than 1%) is photoactivated or photoconverted using a brief pulse of ultraviolet or violet light to render that subset fluorescent. The activated molecules are then imaged and precisely localized followed by photobleaching to remove the unactivated molecules. The process is repeated many thousand times until all of the labeled molecules are obtained which allow the construction of super-resolution images [36]. One example of photoconvertible fluorescent protein is mEosFP which can be photoconverted from green to red fluorescence by 400 nm light [38].

First applications of PALM in filamentous fungi revealed a dynamic picture of the membrane-associated polarity marker TeaR in *A. nidulans* [39]. The PALM analyses clearly showed TeaR clusters near the apex of the hyphae, along the plasma membrane, with average sizes of approximately 120 nm. It was estimated that about 20 TeaR proteins composed each of these clusters. Another PALM example is chitin synthase ChsB in *A. nidulans* [40]. ChsB is mainly located at the Spitzenkörper near the hyphal tip and produces chitin, a key component of the cell wall. The quantitative and time-lapse PALM visualized the pulsatory dynamics of the Spitzenkörper, reflecting vesicle accumulation before exocytosis and their subsequent fusion with the apical plasma membrane [41, 42]. Similar PALM analyses contribute to reveal a MT guidance mechanism depending on actin cables by MigA in *A. nidulans*, an ortholog of the karyogamy protein Kar9 from *Saccharomyces cerevisiae* [43], and dynamics of actin cables in *A. nidulans* [44].

In this chapter, we describe mEosFP based PALM application to the large protein complex, the microtubule organizing center (MTOCs), in *A. nidulans*. Through quantifying the numbers of MztA, GcpC, GcpD and ApsB, we revealed that their molecular numbers at SPBs and sMTOCs are very dynamic (Fig. 5a, b). GcpC is the essential component of γ -TuRCs and each γ -TuRC contains 13–14 γ -tubulin and 6–7 GcpC molecules. We observed different numbers of GcpC molecules at different MTOCs. Interestingly, the numbers differed by 6–7 or multiples of that. Taking into account that each γ -TuRC contains 6–7 GcpC molecules, these results suggested different numbers of entire γ -TuRCs or entire γ -TuSCs at different MTOCs during interphase (Fig. 5c). During metaphase, GcpC numbers (around 60) at SPBs appeared to be constant, suggesting inner plaque nucleation centres are constant to ensure proper assembly of spindles (Fig. 5c).

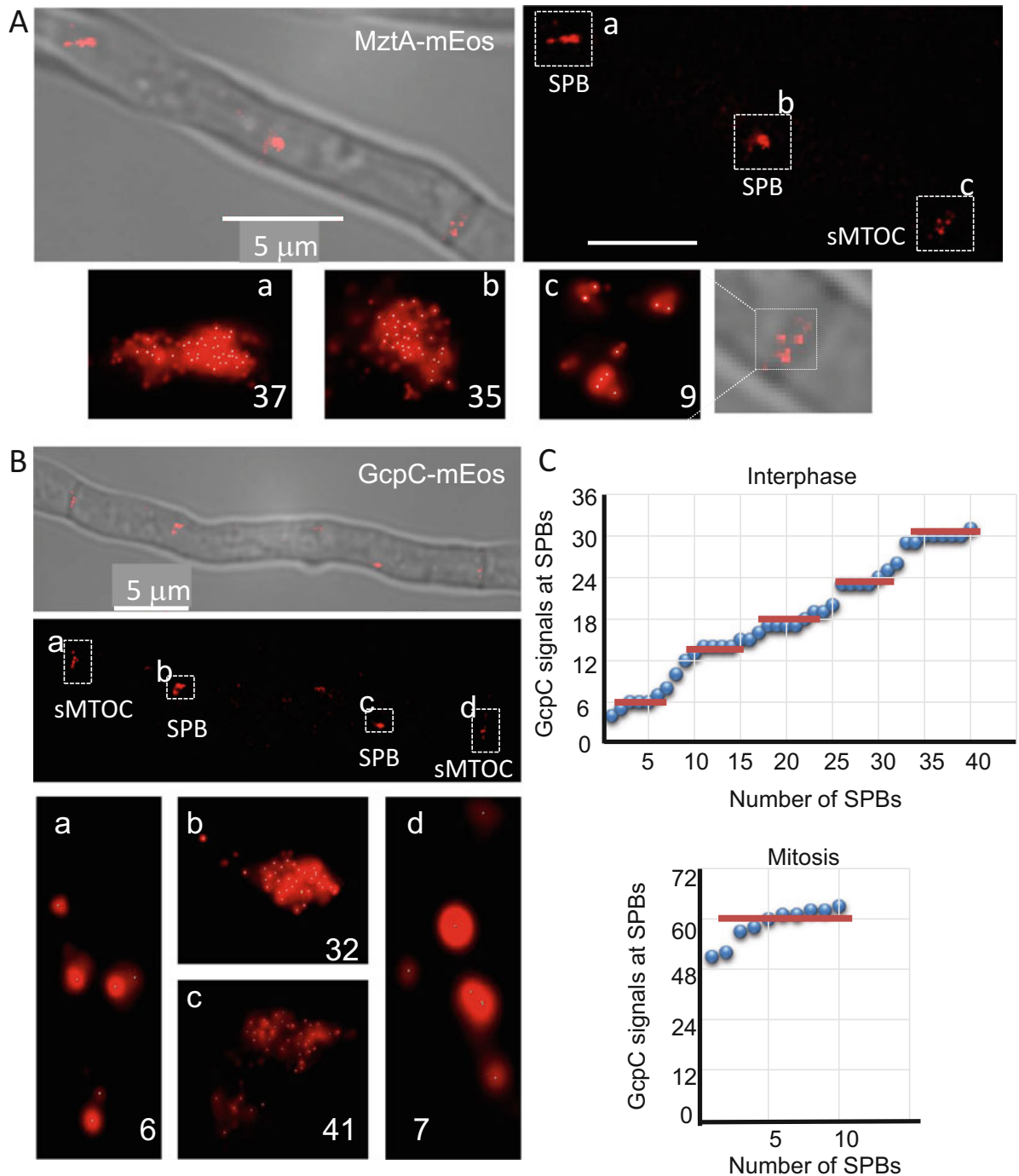


Fig. 5 PALM microscopy images of MztA-mEos and GcpC-mEos at two MTOC sites. (a, b) Images of MztA-mEos (a) and GcpC-mEos (b) at two distinct SPBs and two sMTOCs. Scale bar, 5 μm . (c) GcpC numbers are dynamic in interphase and stable in metaphase. A total of 40 SPBs in interphase and ten SPBs during mitosis were included in the distribution analysis. The numbers of GcpC molecules per SPB were sorted ascendingly. The red line highlights discrete steps of GcpC numbers (Adapted from [22])

This is the first direct evidence for changing numbers of γ -TuRCs/ γ -TuSCs in filamentous fungi during interphase of the cell cycle and shows the power of PALM imaging. PALM imaging allows determination of the number of single molecule and is a

powerful tool to answer the questions of dynamics of individual molecular building blocks as well as elucidating stoichiometry of functional protein complexes in live cells.

2 Materials

2.1 Preparing Hyphae for Live Cell Imaging

1. Minimal medium: 5% (v/v) salt solution, 0.1% (v/v) trace elements, 2% (w/v) glucose or 2% (v/v) glycerol (*see Note 1*), add H₂O_{bid.}, adjust pH with 10 M NaOH to 6.5.
2. Salt solution: 12% NaNO₃, 1% KCl, 1% MgSO₄·7H₂O, 3% KH₂PO₄, add H₂O_{bid.}
3. Trace elements: 2.2% ZnSO₄ x 7H₂O, 1.1% H₃BO₃, 0.5% MnCl₂ x 4H₂O, 0.5% FeSO₄·7H₂O, 0.16% CoCl₂·5H₂O, 0.16% CuSO₄·5H₂O, 0.11% (NH₄)₆Mo₇O₂₄·4H₂O, 5% Na₄-EDTA, adjust pH with 10 M KOH to 6.5.
4. U-slide 8-well glass-bottom dishes for time-lapse images.
5. Strains: SXL36 (*mztA::GFP; alcA(p)::mCherry::tubA*); SXL85 (*mztA::mEoSFP*); SXL98 (*gcpC::mEoSFP*).

2.2 General Microscopy Equipment for Live Cell Imaging

1. Widefield-fluorescence microscope, AxioImager Z1 (Zeiss, Jena, Germany).
2. TL Halogen lamp HXP 120 for excitation of eGFP (488 nm/50 or 100 mW) or mCherry (561 nm/50 or 150 mW).
3. Filter sets: eGFP BP 470/40, FT 495, BP 525/50 and mCherry BP 545/25, FT 570, FT 570, BP 605/70 (Zeiss, Jena, Germany).
4. Zeiss objectives: Plan-Apochromat (63×, NA 1.4).
5. Zeiss AxioCam MR camera.
6. Zeiss software package, Axio Vision v4.8.1, ZEN 2012 Blue Edition v1.20.
7. Microscope slides 76 × 26 mm, 1 mm thickness.
8. Coverslips 18 × 18 mm # 1.

2.3 PALM Set-Up

1. Super-resolution PALM/STROM inverted microscope (ELYRA 3D-PALM, Zeiss, Jena, Germany).
2. High numerical aperture oil immersion objective (α-plan-Apochromat, 100×, numerical aperture, 1.46).
3. Multiple excitation laser lines (405, 473, and 561 nm).
4. An electron-multiplying charge-coupled device (EMCCD) camera (iXon Ultra 897; Andor Technology, Ltd., Belfast, Northern Ireland).
5. Zeiss software package.

3 Methods

To enable live cell imaging in a fungal model system, construction of transgenic strains expressing the proteins of interest fused N- or C-terminally to fluorescent proteins (e.g., the green and red fluorescent protein; eGFP or mCherry) is the first step. In this chapter, MTOC components were all tagged with GFP or mEosFP C-terminally via integration at the endogenous locus (knock-in). Therefore, the fusion proteins are expressed from their natural promoter to avoid overexpression artefacts. Construction details are described here [22]. We also verified that the fusion proteins are biologically functional and do not cause any defective phenotype. For nonessential genes such as *mztA*, which causes a mutant phenotype, the test can be easily done by complementation of the deletion mutant with the construct of interest. Full complementation of the mutant phenotype is desired.

3.1 Live Cell Imaging of MTOC Components in *A. nidulans*

1. Inoculate spores from strain of MztA-GFP; mCherry-tubA into 0.5 ml minimal medium (about 10^3 spores/ml) with 2% glycerol mounted on a sterile coverslip. Incubate the cells for 16–20 h at 28 °C for germination and hyphal growth (*see Note 2*).
2. Mount the coverslips upside down on a microscope slide and avoid air bubbles inside (*see Note 3*).
3. For observation use the 63x objective and an appropriate camera to visualize the whole hyphae.
4. Choose appropriate illumination for excitation of fluorophores, filter sets (excitation/emission/dichroic beam splitter), and exposure time (*see Note 4*).
5. Set up a Z-stack series to get a full set of images according to the thickness of the hyphae (*see Note 5*).
6. Use camera in stream mode to obtain fastest acquisition.
7. Convert resulting images into maximum projection. This results in a 2D projection of 3D data (Fig. 4).
8. Alternatively, quantification of signal intensities between wild type and mutant can be performed (*see Note 6*).

3.2 PALM Experiments

1. Inoculate spores of *A. nidulans* strains expressing GcpC-mEos or MztA-mEos under natural promoter in a glass-bottom chamber with minimal media. Incubate at 25 °C for 12 h.
2. With low 473 nm illumination, identify a cell that expresses a high level of fluorophores.
3. Adjust laser intensity to image mEos. Initially, illuminate the sample with the 561 nm laser to bleach the small population of mEos that is already converted, for example, emits red fluorescence (*see Note 7*).

4. Fluorescent proteins are converted one by one from their green to their red emitting forms using low intensity 405 nm light and excited at 561 nm simultaneous illumination.
5. Use a 607/50 band-pass filter after passing through the excitation dichroic (λ 405/473/561/635) to detect the red fluorescence.
6. Detect and record the signals from individual red fluorescent mEosFP molecules with a back illuminated EMCCD camera typically at 50 ms time resolution (*see Note 8*).
7. Analyse the PALM data with Zen software with PALM method (*see Note 9*). Use the molecule identification and quantification IMARIS 9 \times 64 9.3 software (BITPLANE) alternatively.

4 Notes

1. For choosing the appropriate carbon source in microscopy medium, one has to consider that glucose represses the expression of *alcA* promoter and glycerol de-represses the expression. In another point, glucose helps strains grow faster than glycerol but increases the darkness of the medium. In this chapter, strains are controlled with native promoters; thus, glucose and glycerol are both applied. Considering better visibility, glycerol has priority.
2. For time-lapse images, use glass bottom dishes and hyphae will stay healthy for an extended period of time.
3. After overnight incubation, samples are taken out and put at room temperature for half an hour to adapt to room temperature. Fluorescent protein can be visualized better at room temperature than at 28 °C.
4. We recommend exposure times no longer than 100 ms for eGFP and 200 ms for mCherry. Check the frame rate limit of the camera and choose an appropriate region of interest.
5. Before performing Z-stack images, the center of the hyphae should be focused through the DIC channel to assure that acquisition started in the correct focal plane.
6. Identify a background region of a certain size that can be used in all experiments to correct for background artifacts. Number of Z-stack series should be maintained for all the running and not exceed 20. Shuttle level, laser intensities, and exposure time should be set up identically. One should try to reduce the fluorescence photobleaching as much as possible. Replicates of the experiments need to be done to create data set.
7. A small population of mEosFP emits red fluorescence already before irradiation with 405 nm light. That is typical for mEos.

8. As the pool of nonconverted mEosFP is depleted during data acquisition, it is advisable to increase the power of the activation laser to keep the number of activated fluorophores per frame constant.
9. The PALM micrograph in Fig. 5a is constructed by 1000 frames with a time resolution of 50 ms. ZEN 2.1, use PALM method, settings; discard overlapping molecules. Peak finder; peak mask size, 9 pixel, peak intensive to noise, 6. Localizer; x, y 2D Gauss Fit. Pixel resolution $X\gamma$; 83 nm/pixel.

Acknowledgments

Our research was in part financed by grants from the German Science Foundation (DFG Fi 459/20-1) and Japan Science and Technology Agency (JST, ERATO JPMJER1502).

References

1. Takeshita N, Manck R, Grün N, de Vega SH, Fischer R (2014) Interdependence of the actin and the microtubule cytoskeleton during fungal growth. *Curr Opin Microbiol* 20:34–41
2. Takeshita N (2016) Coordinated process of polarized growth in filamentous fungi. *Biosci Biotechnol Biochem* 80(9):1693–1699
3. Riquelme M, Aguirre J, Bartnicki-García S, Braus GH, Feldbrügge M, Fleig U, Hansberg W, Herrera-Estrella A, Kämper J, Kück U (2018) Fungal morphogenesis, from the polarized growth of hyphae to complex reproduction and infection structures. *Microbiol Mol Biol Rev* 82(2):e00068–e00017
4. Fischer R, Zekert N, Takeshita N (2008) Polarized growth in fungi—interplay between the cytoskeleton, positional markers and membrane domains. *Mol Microbiol* 68(4):813–826
5. Oakley CE, Oakley BR (1989) Identification of γ -tubulin, a new member of the tubulin superfamily encoded by *mipA* gene of *Aspergillus nidulans*. *Nature* 338(6217):662
6. Morris NR, Enos AP (1992) Mitotic gold in a mold: *Aspergillus* genetics and the biology of mitosis. *Trends Genet* 8(1):32–33
7. Osmani SA, Engle DB, Doonan JH, Morris NR (1988) Spindle formation and chromatin condensation in cells blocked at interphase by mutation of a negative cell cycle control gene. *Cell* 52(2):241–251
8. Osmani AH, McGuire SL, Osmani SA (1991) Parallel activation of the NIMA and p34cdc2 cell cycle-regulated protein kinases is required to initiate mitosis in *A. nidulans*. *Cell* 67(2):283–291
9. Horio T, Oakley BR (2005) The role of microtubules in rapid hyphal tip growth of *Aspergillus nidulans*. *Mol Biol Cell* 16(2):918–926
10. Taheri-Talesh N, Horio T, Araujo-Bazán L, Dou X, Espeso EA, Peñalva MA, Osmani SA, Oakley BR (2008) The tip growth apparatus of *Aspergillus nidulans*. *Mol Biol Cell* 19(4):1439–1449
11. Takeshita N, Higashitsuji Y, Konzack S, Fischer R (2008) Apical sterol-rich membranes are essential for localizing cell end markers that determine growth directionality in the filamentous fungus *Aspergillus nidulans*. *Mol Biol Cell* 19(1):339–351
12. Higashitsuji Y, Herrero S, Takeshita N, Fischer R (2009) The cell end marker protein TeaC is involved in growth directionality and septation in *Aspergillus nidulans*. *Eukaryot Cell* 8(7):957–967
13. Jaspersen SL, Winey M (2004) The budding yeast spindle pole body: structure, duplication, and function. *Annu Rev Cell Dev Biol* 20:1–28
14. Cavanaugh AM, Jaspersen SL (2017) Big lessons from little yeast: budding and fission yeast centrosome structure, duplication, and function. *Annu Rev Genet* 51:361–383
15. Knop M, Schiebel E (1997) Spc98p and Spc97p of the yeast γ -tubulin complex mediate binding to the spindle pole body via their interaction with Spc110p. *EMBO J* 16(23):6985–6995

16. Liu P, Zupa E, Neuner A, Böhler A, Loerke J, Flemming D, Ruppert T, Rudack T, Peter C, Spahn C, Gruss OJ, Pfeffer S, Schiebel E (2020) Insights into the assembly and activation of the microtubule nucleator γ -TuRC. *Nature* 578(7795):467–471
17. Xiong Y, Oakley BR (2009) In vivo analysis of the functions of γ -tubulin-complex proteins. *J Cell Sci* 122(22):4218–4227
18. Heitz MJ, Petersen J, Valovin S, Hagan IM (2001) MTOC formation during mitotic exit in fission yeast. *J Cell Sci* 114(24):4521–4532
19. Höög JL, Schwartz C, Noon AT, O'Toole ET, Mastronarde DN, McIntosh JR, Antony C (2007) Organization of interphase microtubules in fission yeast analyzed by electron tomography. *Dev Cell* 12(3):349–361
20. Konzack S, Rischitor PE, Enke C, Fischer R (2005) The role of the kinesin motor KipA in microtubule organization and polarized growth of *Aspergillus nidulans*. *Mol Biol Cell* 16(2):497–506
21. Zekert N, Veith D, Fischer R (2010) Interaction of the *Aspergillus nidulans* microtubule-organizing center (MTOC) component ApsB with gamma-tubulin and evidence for a role of a subclass of peroxisomes in the formation of septal MTOCs. *Eukaryot Cell* 9(5):795–805
22. Gao X, Schmid M, Zhang Y, Fukuda S, Takeshita N, Fischer R (2019) The spindle pole body of *Aspergillus nidulans* is asymmetrical and contains changing numbers of γ -tubulin complexes. *J Cell Sci* 132(24):jcs234799
23. Zhang Y, Gao X, Manck R, Schmid M, Osmani AH, Osmani SA, Takeshita N, Fischer R (2017) Microtubule-organizing centers of *Aspergillus nidulans* are anchored at septa by a disordered protein. *Mol Microbiol* 106(2):285–303
24. Samejima I, Lourenço PC, Snaith HA, Sawin KE (2005) Fission yeast mto2p regulates microtubule nucleation by the centrosome-related protein mto1p. *Mol Biol Cell* 16(6):3040–3051
25. Samejima I, Miller VJ, Rincon SA, Sawin KE (2010) Fission yeast Mto1 regulates diversity of cytoplasmic microtubule organizing centers. *Curr Biol* 20(21):1959–1965
26. Flory MR, Morphew M, Joseph JD, Means AR, Davis TN (2002) Pcp1p, an Spc110p-related calmodulin target at the centrosome of the fission yeast *Schizosaccharomyces pombe*. *Cell Growth Differ* 13(2):47–58
27. Hutchins JR, Toyoda Y, Hegemann B, Poser I, Hériché J-K, Sykora MM, Augsburg M, Hudecz O, Buschhorn BA, Bulkescher J (2010) Systematic analysis of human protein complexes identifies chromosome segregation proteins. *Science* 328(5978):593–599
28. Tovey CA, Tubman CE, Hamrud E, Zhu Z, Dyas AE, Butterfield AN, Fyfe A, Johnson E, Conduit PT (2018) γ -TuRC heterogeneity revealed by analysis of Mozart1. *Curr Biol* 28(14):2314–2323.e2316
29. Schermelleh L, Ferrand A, Huser T, Eggeling C, Sauer M, Biehlmaier O, Drummen GP (2019) Super-resolution microscopy demystified. *Nat Cell Biol* 21(1):72–84
30. Sigal YM, Zhou R, Zhuang X (2018) Visualizing and discovering cellular structures with super-resolution microscopy. *Science* 361(6405):880–887
31. Nordzike S, Zobel T, Fränzel B, Wolters DA, Kück U, Teichert I (2015) A fungal sarcolemmal membrane-associated protein (SLMAP) homolog plays a fundamental role in development and localizes to the nuclear envelope, endoplasmic reticulum, and mitochondria. *Eukaryot Cell* 14(4):345–358
32. Dempwolff F, Schmidt FK, Hervás AB, Stroth A, Rösch TC, Riese CN, Dersch S, Heimerl T, Lucena D, Hülsbusch N (2016) Super resolution fluorescence microscopy and tracking of bacterial flotillin (Reggie) paralogs provide evidence for defined-sized protein microdomains within the bacterial membrane but absence of clusters containing detergent-resistant proteins. *PLoS Genet* 12(6):e1006116
33. Takeshita N, Diallinas G, Fischer R (2012) The role of flotillin FloA and stomatin StoA in the maintenance of apical sterol-rich membrane domains and polarity in the filamentous fungus *Aspergillus nidulans*. *Mol Microbiol* 83(6):1136–1152
34. Chen F, Tillberg PW, Boyden ES (2012) Expansion microscopy. *J Phys Oceanogr* 42:1445–1460
35. Götz R, Panzer S, Trinks N, Eilts J, Wagener J, Turrà D, Di Pietro A, Sauer M, Terpitz U (2020) Expansion microscopy for cell biology analysis in fungi. *Front Microbiol* 11:574
36. Betzig E, Patterson GH, Sougrat R, Lindwasser OW, Olenych S, Bonifacino JS, Davidson MW, Lippincott-Schwartz J, Hess HF (2006) Imaging intracellular fluorescent proteins at nanometer resolution. *Science* 313(5793):1642–1645
37. Sahl SJ, Moerner W (2013) Super-resolution fluorescence imaging with single molecules. *Curr Opin Struct Biol* 23(5):778–787
38. Wiedenmann J, Gayda S, Adam V, Oswald F, Nienhaus K, Bourgeois D, Nienhaus GU

- (2011) From EosFP to mIrisFP: structure-based development of advanced photoactivatable marker proteins of the GFP-family. *J Biophotonics* 4(6):377–390
39. Ishitsuka Y, Savage N, Li Y, Bergs A, Grün N, Kohler D, Donnelly R, Nienhaus GU, Fischer R, Takeshita N (2015) Superresolution microscopy reveals a dynamic picture of cell polarity maintenance during directional growth. *Sci Adv* 1(10):e1500947
 40. Zhou L, Evangelinos M, Wernet V, Eckert AF, Ishitsuka Y, Fischer R, Nienhaus GU, Takeshita N (2018) Superresolution and pulse-chase imaging reveal the role of vesicle transport in polar growth of fungal cells. *Sci Adv* 4(1):e1701798
 41. Takeshita N, Evangelinos M, Zhou L, Serizawa T, Somera-Fajardo RA, Lu L, Takaya N, Nienhaus GU, Fischer R (2017) Pulses of Ca²⁺ coordinate actin assembly and exocytosis for stepwise cell extension. *Proc Natl Acad Sci U S A* 114(22):5701–5706
 42. Takeshita N (2018) Oscillatory fungal cell growth. *Fungal Genet Biol* 110:10–14
 43. Manck R, Ishitsuka Y, Herrero S, Takeshita N, Nienhaus GU, Fischer R (2015) Genetic evidence for a microtubule-capture mechanism during polarised growth of *Aspergillus nidulans*. *J Cell Sci* 128(19):3569–3582
 44. Bergs A, Ishitsuka Y, Evangelinos M, Nienhaus G, Takeshita N (2016) Dynamics of actin cables in polarized growth of the filamentous fungus *Aspergillus nidulans*. *Front Microbiol* 7:682